Water Permeability and Mechanical Strength of Polyunsaturated Lipid Bilayers

K. Olbrich,* W. Rawicz,† D. Needham,* and E. Evans†‡

*Department of Mechanical Engineering and Materials Science, Duke University, Durham, North Carolina 27708-0300 USA; †Department of Pathology, University of British Columbia, Vancouver, British Columbia V6T 1W5, Canada; and ‡Department of Physics, University of British Columbia, Vancouver, British Columbia V6T 1Z1, Canada

ABSTRACT Micropipette aspiration was used to test mechanical strength and water permeability of giant-fluid bilayer vesicles composed of polyunsaturated phosphatidylcholine PC lipids. Eight synthetic-diacyl PCs were chosen with 18 carbon chains and degrees of unsaturation that ranged from one double bond (C18:0/1, C18:1/0) to six double bonds per PC molecule (diC18:3). Produced by increasing pipette pressurization, membrane tensions for lysis of single vesicles at 21°C ranged from ~9 to 10 mN/m for mono- and dimono-unsaturated PCs (18:0/1, 18:1/0, and diC18:1) but dropped abruptly to ~5 mN/m when one or both PC chains contained two *cis*-double bonds (C18:0/2 and diC18:2) and even lower ~3 mN/m for diC18:3. Driven by osmotic filtration following transfer of individual vesicles to a hypertonic environment, the apparent coefficient for water permeability at 21°C varied modestly in a range from ~30 to 40 μm/s for mono- and dimono-unsaturated PCs. However, with two or more *cis*-double bonds in a chain, the apparent permeability rose to ~50 μm/s for C18:0/2, then strikingly to ~90 μm/s for diC18:2 and ~150 μm/s for diC18:3. The measurements of water permeability were found to scale exponentially with the reduced temperatures reported for these lipids in the literature. The correlation supports the concept that increase in free volume acquired in thermal expansion above the main gel-liquid crystal transition of a bilayer is a major factor in water transport. Taken together, the prominent changes in lysis tension and water permeability indicate that major changes occur in chain packing and cohesive interactions when two or more *cis*-double bonds alternate with saturated bonds along a chain.

INTRODUCTION

The majority of phospholipid acyl chains in animal cell membranes are saturated (only C—C bonds) or monounsaturated (one C═C bond) hydrocarbon polymers. Consequently, phospholipid bilayers with saturated or monounsaturated chains have been studied extensively, which includes the gel-to-liquid crystalline phase transitions that are prominent for saturated PC bilayers above 0°C in aqueous environments. Interestingly, to ensure that membranes of eukaryotic cells remain fluid (yet maintain strong, nearly impermeable interfaces), nature seems to have preferred cholesterol as a co-constituent even though polyunsaturation can also keep bilayers fluid to below water freezing temperatures. A simple rationale for not choosing polyunsaturated lipids is that they oxidize easily and would be chemically expensive to keep in membranes. But surprisingly, there are membranes rich in polyunsaturated lipids, as in brain tissue. Lipid polyunsaturation is not the only distinguishing feature of these special membranes; there are usually significant variations in chain lengths and differences in cholesterol content. Even so, we are compelled to ask how such labile and exotic lipids affect the material characteristics of membranes? Here, we report measurements of dynamic material properties—mechanical rupture strength and water permeability—of fluid diacyl phosphatidylcholine PC bilayers with equal chain lengths of 18 carbons and a wide range of unsaturation (1, 2, 4, or 6 double bonds per lipid). In a companion article (Rawicz et al., 2000), we present measurements of equilibrium elastic—and thickness—properties of the same PC bilayers. In both studies, we have used micropipette aspiration methods to directly measure membrane mechanical properties and permeability to water on giant-single bilayer vesicles. In this study, the results show that polyunsaturated PC bilayers are much more permeable and much weaker than the prototypical monounsaturated lipid bilayer.

Several techniques have been used to quantitate mechanical stretch properties of bilayers, which include the micropipette approach we have pioneered for giant vesicles (Kwok and Evans, 1981; Evans and Needham, 1987), photon correlation spectroscopy and dynamic light scattering of small vesicles under osmotic stress (Rutkowski et al., 1991; Hallett et al., 1993), cryoelectron microscopy of vesicles subjected to osmotic stress (Mui et al., 1993), nuclear magnetic resonance NMR and x-ray diffraction of strongly dehydrated multibilayer arrays (Koenig et al., 1997), plus others. Of these approaches, only the micropipette method can provide measurements of bilayer stretch on a single vesicle with a resolution of better than 0.1% relative change in area, test elasticity and reversibility, plus determine instantaneous tension and area dilation at rupture. In comparison to mechanical properties, permeability of bilayers to water has a long history embodied in numerous references describing a variety of measurements from osmotic filtration to isotope diffusion (Finkelstein, 1987, covers many of

Received for publication 1 October 1999 and in final form 28 March 2000.

Address reprint requests to Dr. Evan Evans, Dept. of Physics, University of British Columbia, Vancouver, BC V6T 1Z1, Canada. Tel.: 604-822-7103; Fax: 604-822-7635; E-mail: evans@physics.ubc.ca. email: evans@physics.ubc.ca.

0006-3495/00/07/321/07 $2.00

the important concepts and early work; recent contributions include Paula et al., 1996, and Huster et al., 1997). A prominent feature of water permeability measurements has been the significant variation in values obtained by different techniques and different laboratories. For instance, in early work on permeability of egg PC bilayers (similar to C18:0/1 PC tested here), the values of water permeability ranged from 10 to 50 μm/s (Fettiplace and Haydon, 1980). Likewise, permeability coefficients for osmotic filtration in some studies exceeded the values of permeability derived from tracer diffusion (Jansen and Blume, 1989) whereas in others, no difference was found between results with the two methods (Finkelstein, 1987; Ye and Verkman, 1989). More than experimental aesthetics, careful comparison of these two types of permeability measurement is expected to reveal important insights as to the mechanism of transport (Finkelstein, 1987; Paula et al., 1996; Xiang and Anderson, 1997). In our tests, the goal has been to expose the impact of polyunsaturation on permeability of single bilayers to water. Our approach has been to use micropipette aspiration of giant unilamellar vesicles and manipulation into a hyperosmotic environment as a simple technique to measure water filtration. The unique feature of the method is that it provides direct observation of water filtration across a single solvent-free and unsupported bilayer, which can be easily analyzed to obtain the coefficient for bilayer permeability to water.

MATERIALS AND METHODS

Lipids

Eight synthetic species of diacyl C18 PC lipids were obtained from Avanti Polar Lipids (Alabaster, AL) in chloroform and used without further purification. Seven were *cis* unsaturated: 1-stearoyl-2-oleoyl-*sn*-glycero-3-phosphocholine (C18:0/1_{c9}); 1-oleoyl-2-stearoyl-*sn*-glycero-3-phosphocholine (C18:1_{c9}/0); 1,2-dipetroselinoleoyl-*sn*-glycero-3-phosphocholine (diC18:1_{c6}); 1,2-dioleoyl-*sn*-glycero-3-phosphocholine (diC18:1_{c9}); 1-stearoyl-2-linoleoyl-*sn*-glycero-3-phosphocholine (C18:0/$2_{c9,12}$); 1,2-dilinoleoyl-*sn*-glycero-3-phosphocholine (diC18:$2_{c9,12}$); and 1,2-dilinolenoyl-*sn*-3-phosphatidylcholine (diC18:$3_{c9,12,15}$). One was *trans* unsaturated: 1,2-elaidoyl-*sn*-glycero-3-phosphocholine (diC18:1_{t9}). The solutions were placed in amber glass screw-cap vials with Teflon-lined silicone septa. Especially important for the preservation of the oxidation-prone fatty acid chains (C18:0/2, diC18:2, and diC18:3), the vials were wrapped in aluminum foil and stored at −20°C under argon.

Vesicle preparation and assay of lipid oxidation

In our laboratories, the generic procedure for preparation of giant vesicles (15–30 μm diameter) is to rehydrate lipid films dried first from chloroform/methanol (2:1) onto the surface of a roughened Teflon disk (Needham et al., 1988). After deposition of the lipid film and evaporation of the organic solvent in vacuo, the Teflon disk is covered with a warm (37°C) sucrose solution (200 mOsm) and allowed to hydrate. To create a refractive index contrast between inside/outside of vesicles and to sediment vesicles in the microscope chamber, an aliquot of vesicles is diluted manyfold in an equiosmolar solution of glucose or electrolyte buffer. The refractive index gradient is used to enhance optical detection of the projection length inside the pipette as shown by the example in Fig. 1. Described below, accurate video tracking of the projection edge enables discrimination of $<0.1\%$ relative change in vesicle area or volume, even though optical measurements of total area and volume remain limited to a few percent accuracy by diffraction. For formation of vesicles from polyunsaturated lipids, slight modifications were made in the procedure. First, argon-purged, deionized water was used to make the hydration and suspension solutions. Second, the container with the polyunsaturated lipid film was wrapped in aluminum foil (to minimize exposure to light). The polyunsaturated lipids were allowed to hydrate for only three hours under argon and used immediately (normally, lipids are left to hydrate overnight then used the next day). At the beginning of the study, samples of the polyunsaturated lipids were tested for possible oxidative damage over the time scales associated with preparation and experiment by spectrophotometric assay (Kim and LaBella, 1987; New, 1990). The absorbance of a solution of 1 mM lipid in absolute ethanol was measured at ~230 nm using a Beckman DU-7500 diode-array spectrophotometer (Beckman, Fullerton, CA). Absorption at this wavelength indicated the presence of conjugated dienes in the hydrocarbon chain, which result from oxidation (Kim and LaBella, 1987; New, 1990). Lipid samples used soon after arrival from Avanti showed no detectable oxidative damage. Moreover, measurements of properties repeated with preparations from the same polyunsaturated lipid samples and from new samples purchased at later times gave identical results.

Mechanical expansion and rupture of vesicle bilayers

Micropipette suction was used to pressurize vesicles and stretch bilayers to rupture. Well-established from mechanics (Kwok and Evans, 1981), suction pressure P applied to a fluid-bilayer vesicle produces a uniform membrane tension τ_m, which is described by a simple geometric relation based on the pipette caliber (diameter) D_p and diameter D_v of the vesicle-spherical segment exterior to the pipette, i.e.,

$$\tau_m = PD_p/4(1 - D_p/D_v)$$

The pipette suction (~10^3 Pa) needed to expand the area of a ~20 μm vesicle is small compared to osmotic driving forces (~10^5 Pa) required to kinetically displace water on the time scale of the experiment and small compared to the osmotic activity of the trapped sucrose (~5×10^5 Pa). Thus, vesicle volume remains effectively fixed in the area expansion test. Increase of the aspirated projection length L_p inside the pipette provides a direct measure of the area expansion. Precise changes in area ΔA with displacement ΔL_p of the projection length in experiments were computed numerically as described in the Appendix. The proportionality between area and length is easily seen in the following first-order approximation:

$$\Delta A \approx \pi D_p(1 - D_p/D_v)\Delta L_p$$

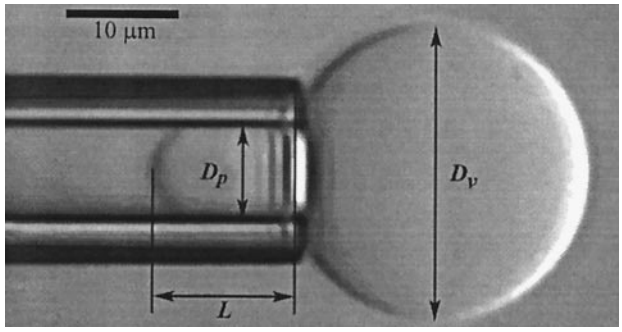

FIGURE 1 Video micrograph of a single bilayer vesicle (diameter ~20 μm) held by micropipette suction.

Backed by this analysis, the following simple procedure was used to test membrane strength and maximum dilation. The vesicle was first prestressed under a tension of ~0.5 mN/m to incorporate hidden-excess area. Then, pipette suction was increased in steps—each held steady for several seconds—until lysis occurred (total pressurization time of <1 min) at pressures of ~1–5 × 10^3 Pa, where tensions reached the range of 3–10 mN/m for lysis, depending on the lipid.

Osmotic filtration of water from single vesicles

To measure bilayer permeability to water, single vesicles were selected by a micropipette and transferred to an adjacent microscope chamber with ~10% higher solute concentration. In the new environment, water was driven out of the vesicle by strong osmotic forces (>10^5 Pa) to achieve equilibrium. The time course of vesicle dehydration was tracked and analyzed to obtain the transport coefficient for water filtration. To transfer a vesicle through the small air gap that separated the microscope chambers, the vesicle was maneuvered into the entrance of another larger pipette. The microscope stage was then translated to leave the sheltered vesicle in the second chamber, where it was brought out into the new environment. Typically, vesicles were transferred from a chamber that contained a 200 mOsm glucose solution to a chamber that contained a hypertonic (220 mOsm) glucose solution. However, specific tests were also performed at twofold higher osmolarities to verify the expected proportionality between filtration rate and level of osmolarity. Transfer back to the original chamber was used to verify that the water exchange was recoverable and that no sucrose solute escaped or glucose solute entered the vesicle. Throughout the test, the vesicle was held under small fixed suction pressure to control bilayer tension (~1 mN/m). Thus, changes in vesicle volume occurred at constant area and were computed precisely from displacements of the projection length inside the pipette, as described in the Appendix. The proportionality between change in volume ΔV and displacement ΔL_p of the projection length is demonstrated by the first-order approximation:

$$\Delta V \approx -\pi D_p(D_v - D_p)\Delta L_p/4$$

Displacement of the projection length of an aspirated vesicle under osmotic dehydration is shown in Fig. 2

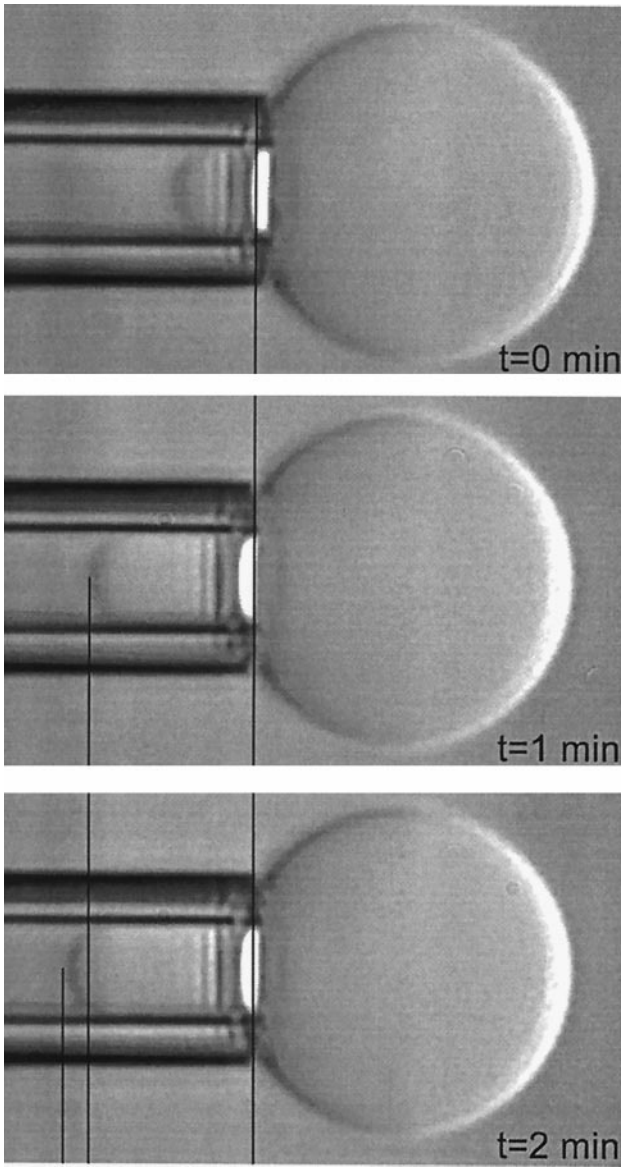

FIGURE 2 Video micrographs of a single bilayer vesicle during the course of dehydration in a water filtration experiment. The increase in aspiration length inside the pipette is proportional to the reduction in vesicle volume.

RESULTS AND ANALYSIS

Water permeability

Measurements of aspiration length versus time after transfer of vesicles to a hypertonic environment were used to quantitate water filtration over the course to a new state of osmotic equilibrium. Fig. 3 shows the time dependence of vesicle dehydration followed by rehydration (when returned to the original chamber), which illustrates both approach to osmotic equilibrium and reversibility. The kinetics of the time course were analyzed with the standard phenomenological law for water transport across a semipermeable membrane and the dilute concentration approximation for osmotic activity (Finkelstein, 1987). As such, the rate of change in vesicle volume per unit of surface area A is governed by the bilayer permeability coefficient P_f and the outside-inside difference Δc in osmolarity, according to

$$1/A(dV/dt) = -(P_f\nu_w)\Delta c$$

where ν_w is the molar volume of water (18 ml/mol). Because the membrane is impermeable to solutes (on the time scale for water filtration), the instantaneous osmolarity of the vesicle interior is set by the number of moles m of solute and the volume, i.e., $c = m/V$. Scaling instantaneous volume by the final equilibrium volume V_∞, we obtain a dimensionless kinetic equation for the time course to the new equilibrium state,

$$dV^*/dt = -P_f c_\infty \nu_w (A/V_\infty)[(V^* - 1)/V^*]$$

with definitions of $V^* = V/V_\infty$ and c_∞ equal to the final osmolarity. Relative to the dimensionless volume V_o^* at time $t = 0$, the time course obeys the following transcendental

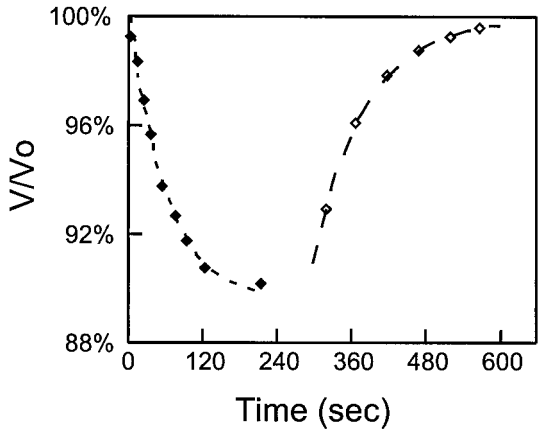

FIGURE 3 Evolution of vesicle volume with time in a water filtration experiment. The first phase shows dehydration in response to transfer from a 200 mOsm glucose solution into a hyperosmotic (220 mOsm) glucose solution. The second phase demonstrates the full recovery of volume after return to the original solution around ~300 s. Here, the vesicle bilayer was composed of C18:0/1 PC and tested at 18°C. From measurements of vesicle dimensions inside and outside the pipette, the area of the vesicle was calculated to be ~1940 μm^2, and the volume was ~11,200 μm^3.

TABLE 1 Rupture tension τ_m^* and apparent permeability P_{fapp} to water measured at 21°C on single-bilayer vesicles made from polyunsaturated PC bilayers

Lipid	τ_m^* (mN/m)	P_{fapp} (μm/sec)	T_m (°C)
C18:0/1	9.0 ± 1.7	28 ± 6	6 (Davis and Keough, 1983)
C18:1/0	10.0 ± 1.8	30 ± 2	9 (Davis and Keough, 1983)
diC18:1_{c9}	9.9 ± 2.6	42 ± 6	−22 (Barton and Gunstone, 1975)
diC18:1_{t9}	8.5 ± 2.0	30 ± 5	12 (Silvius and McElhaney, 1979)
diC18:1_{c6}	9.9 ± 1.9	35 ± 4	1 (Barton and Gunstone, 1975)
C18:0/2	4.9 ± 1.6	49 ± 6	−15 (Keough and Parsons, 1990)
diC18:2	5.1 ± 1.0	91 ± 24	−53 (Keough and Kariel, 1987)
diC18:3	3.1 ± 1.0	146 ± 26	−60 (Keough and Kariel, 1987)

Values are given as mean ± standard deviation. Gel-to-liquid crystalline phase transition temperatures (T_m) reported in the literature for PCs with two 18-carbon chains.

equation:

$$(V^* - 1)\exp(V^*) = (V_o^* - 1)\exp(-k \cdot t + V_o^*)$$

with the time rate of decay set by $k = A(P_f c_\infty \nu_w)/V_\infty$.

Using a nonlinear fitting algorithm, this equation was matched to the time-dependent change in volume of each vesicle tested, which yielded the time constant $1/k$ for approach to osmotic equilibrium. From each value of the decay constant we obtained an *apparent* measure of the permeability coefficient (P_{fapp}). As seen above, the time constant for volume changes scales inversely with the osmolarity of the environment. This intrinsic feature was verified in separate tests where a twofold increase in osmolarity reduced the time constant by exactly a factor of one-half, as expected. Measurements of *apparent* water permeability (P_{fapp}) were performed on at least 10 vesicles for each type of lipid. The results (±SD) are listed in Table 1 and plotted as a histogram in order of increasing unsaturation in Fig. 4. The *apparent* permeabilities were found to increase modestly with mono- and dimono-unsaturation, but incorporation of alternating *cis*-double bonds led to a significant augmentation of permeability. The semi-log plot in Fig. 5 demonstrates that log(*apparent* permeability) varies linearly with the reduced temperature of each lipid relative to the gel-liquid crystalline phase transition temperature reported in the literature (Table 1).

Because of diffusion through unstirred layers adjacent to the bilayer, the prominent increase of permeability seen for the most unsaturated lipids (diC18:2 and diC18:3) was expected to be even more pronounced than revealed by the measurements of P_{fapp}. Conservatively, the added impedance is estimated by the ratio of a diffusion length set by the vesicle radius $R_v = D_v/2$ (~10 μm) to the diffusivity D_w of water (~3×10^3 μm^2/s), which implies that $1/P_{fapp} \approx 1/P_f + R_v/D_w$ (Finkelstein, 1987; Goldstein and Dembo, 1995). Based on this approximation, unstirred layers should be significant for a ~20-μm-size vesicle made from diC18:3 PC because the estimated value of $P_f \sim 284$ μm/s is much larger than the measured value $P_{fapp} \sim 146$ μm/s. To test the

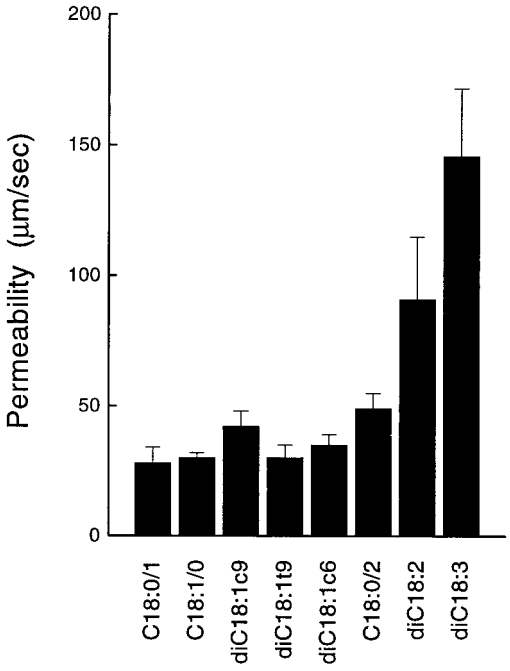

FIGURE 4 Coefficients of *apparent* water permeability for polyunsaturated PC bilayers measured by osmotic filtration at 21°C.

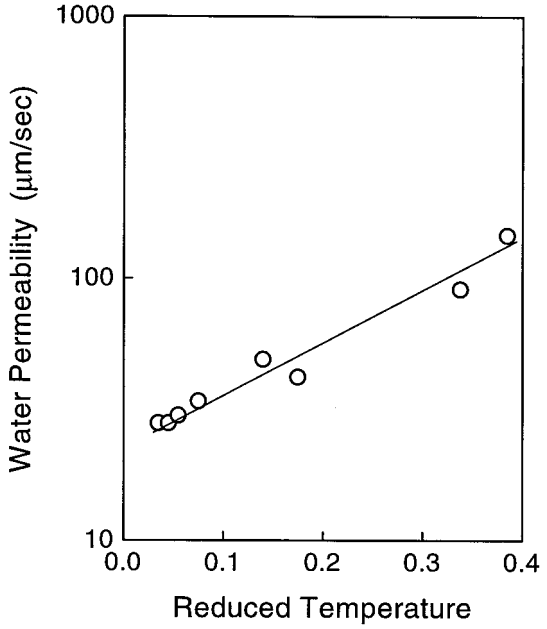

FIGURE 5 Log(*apparent* water permeability) versus reduced temperature $T_r = (T - T_m)/T_m$ for polyunsaturated PCs at 21°C. The reduced temperatures are based on the literature values listed in Table 1 for gel-to-liquid crystalline phase transition temperatures (T_m).

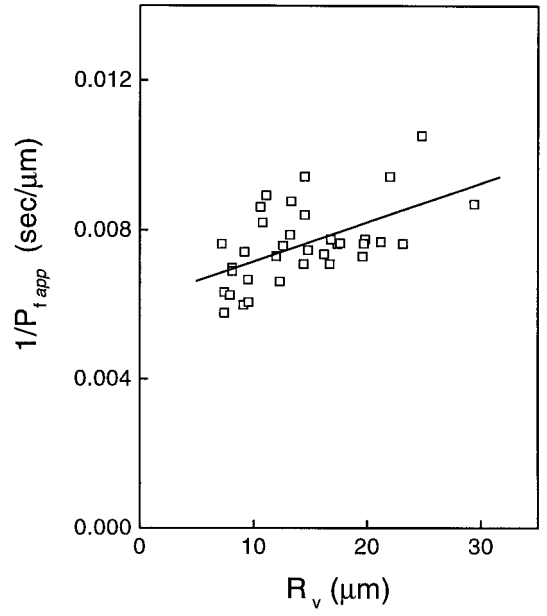

FIGURE 6 Measurements of *apparent* water permeability for single vesicles composed of diC18:3 PC (at 18°C) plotted as a function of vesicle radius. The linear regression line implies the unstirred layer impedance is $\sim 0.0001\ s/\mu m^2 \times R_v$.

significance of unstirred layers, a separate set of experiments was performed where the apparent permeabilities of diC18:3 vesicles were measured over the widest possible range of vesicle sizes $2R_v \sim 15$–$60\ \mu m$. The reciprocal values $1/P_{fapp}$ are plotted as a function of radii in Fig. 6. Surprisingly, the data in Fig. 6 show a more modest increase in apparent permeability with reduction in vesicle size than predicted by the simple model. Based on the linear fit to the data shown in Fig. 6, the unstirred layer impedance was found to be $\sim(0.0001\ s/\mu m^2)R_v$, which is threefold lower than the value given by R_v/D_w. Thus, the permeability coefficients corrected for unstirred layers would increase from $P_{fapp} \sim 90\ \mu m/s$ to $P_f \sim 100\ \mu m/s$ for diC18:2 and from $P_{fapp} \sim 146\ \mu m/s$ to $P_f \sim 170\ \mu m/s$ for diC18:3, with negligible impact on the permeability coefficients measured for the more saturated PCs.

Rupture strength

Ramped upward until the vesicle ruptured, pipette suction was used to establish the tension limit for bilayer strength. The rate of tension loading was ~0.1 mN/m/s. Cumulated from tests of at least 10 vesicles for each lipid type (listed in Table 1), Fig. 7 presents a histogram of the rupture tensions τ_m^* (±SD) for PC bilayers arranged in order of increasing unsaturation. For bilayers with up to one unsaturated-double bond per chain, rupture strength varied little from $\tau_m^* \sim 10$ mN/m. However, rupture tensions of bilayers with two or more alternating *cis*-double bonds (C═C—C═C) in one or both chains dropped precipitously to $\tau_m^* \sim 5$ mN/m for C18:0/2, diC18:2, and even weaker—$\tau_m^* \sim 3$ mN/m—for diC18:3. Moreover, the direct stretch moduli of the bilayers were found to vary by $<\pm 10\%$ from a mean value of $K_A = 243$ mN/m (see Rawicz et al., 2000); so the fractional

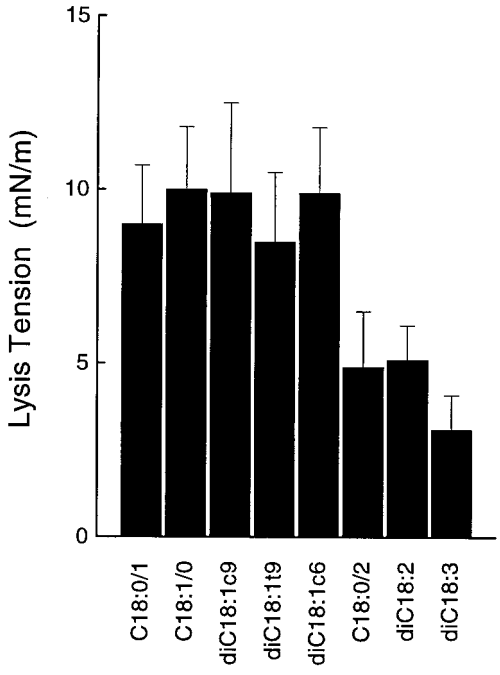

FIGURE 7 Lysis tensions for vesicles with polyunsaturated PC bilayers.

changes in area of bilayers at rupture $\alpha^* = \tau_m^*/K_A$ also dropped commensurately from a value of $\alpha^* \approx 0.04$ to $\alpha^* \approx 0.02$ (or $\alpha^* \approx 0.012$ for diC18:3). Clearly, two or more alternating *cis*-double bonds make the bilayer distinctly weaker than bilayers of mono- and dimono-unsaturated PCs.

DISCUSSION AND CONCLUSIONS

Water permeability

Because of the sensitivity to changes in vesicle volume, aspiration into a micropipette provides a precise method to measure the transport coefficient (permeability) for water filtration across a single bilayer. Tested experimentally, impedance to filtration from unstirred layers was found to be much less ($\sim$0.0001 s/μm^2 $\times$ R_v) than predicted by the ratio of vesicle radius to water diffusivity ($\sim$0.0003 s/μm^2 $\times$ R_v). As such, a bilayer permeability coefficient of $\sim$200 μm/s defines a reasonable upper bound accessible to measurement by the micropipette technique in the absence of some type of convective mixing (e.g., using an auxiliary pipette to blow solution past the vesicle). Calculated from the time course of osmotic filtration for each vesicle, the *apparent* permeabilities at 21°C varied modestly between 28 and 42 μm/s for mono- and dimono-unsaturated PC bilayers. Within this range, there were only subtle variations associated with position and *trans* or *cis* configurations of the double bond. However, the most striking result was that two or more alternating *cis*-double bonds along a chain led to major increase in *apparent* permeability of bilayers to water ($\sim$49 μm/s for C18:0/2, $\sim$90 μm/s for diC18:2, and $\sim$146 μm/s for diC18:3 at 21°C). A similar impact of unsaturation on water permeability was found by Huster et al. (1997). However, their values of permeability coefficient differ significantly from our measurements in Table 1. Using NMR spectroscopy to follow exchange of ^{17}O across membranes of $\sim$100-nm-size vesicles, the measurements of Huster et al. give values of $\sim$123 μm/s for C18:0/1, $\sim$97 μm/s for diC18:1, and $\sim$261 μm/s for the asymmetric C18:0/3 at 21°C. The puzzling feature is the large ($\sim$3-fold) discrepancy between their values and our values for the mono- and dimono-unsaturated PC bilayers under conditions where unstirred layer effects were completely negligible in both types of experiments. A similar discrepancy exists between our measurement of permeability coefficient ($\sim$42 μm/s at 21°C) for diC18:1 and the value of $\sim$150 μm/s obtained by Paula et al. (1996), albeit measured at 30°C. Based on the activation energies for diC18:1 given in Huster et al. (1997), the value at 21°C would only reduce to $\sim$91 μm/s, which remains far from our value of 42 μm/s. In comparison, Finkelstein measured the permeability of planar egg PC bilayers to water at 25°C and obtained a value of $\sim$22 μm/s, which is consistent with the value of $\sim$28 μm/s we found for the closely related C18:0/1 at 21°C. Most intriguing, the values of log(*apparent* permeability) from our measurements yield a linear correlation with the reduced temperatures of these lipids relative to the gel-liquid crystalline phase transition temperatures reported in the literature, as shown in Fig. 5. The exponential rise in permeability with increase in reduced temperature implies that free volume in the hydrocarbon region increases significantly under thermal expansion of area per lipid above the gel-liquid crystalline phase transition. This is consistent with the concept emphasized by Xiang and Anderson (1997) that the partition of solutes (water) in the hydrocarbon region is strongly effected by chain-ordering, which diminishes progressively with reduced temperature in bilayers.

Rupture strength

Measured under a ramp of tension at a rate of $\sim$0.1 mN/m/s, mono- and dimono-unsaturated PC bilayers ruptured at nearly the same level of tension, $\sim$10 mN/m. But as seen in Fig. 7, there was an major drop in bilayer strength to $\sim$3–5 mN/m when the number of unsaturated bonds in one or both hydrocarbon chains was increased from one to two or more. Although these measurements at a single rate provide a comparative assay of bilayer strength, it is important to recognize that strength is a dynamic material property that will change with the period of time subjected to different levels of tension set by tension loading rate. This follows from the accepted view that rupture of a fluid membrane emanates from formation of unstable pores. The theory for rupture pore nucleation was first proposed by Deryagin and Gutop (1962) for breakdown of thin films and is a 2-D version of the classic theory for cavitation in 3-D liquids introduced by Zeldovich (1943) a generation earlier. In this dynamical theory, the membrane is modeled as a simple elastic continuum where the energetics of an open hole (radius r) involve a constant-edge energy ϵ (energy/length) $\times$ hole perimeter $2\pi r$ and the applied mechanical potential τ_m (πr^2) as expressed by $E(r) = (2\pi r)\epsilon - \tau_m(\pi r^2)$. From the model, we see that edge energy is the material property responsible for membrane strength. More subtly, however, membrane rupture is a kinetic process where the events are governed by thermally activated nucleation and thus depend on a tension-mediated energy barrier, $E^* = \pi\epsilon^2/\tau_m$, which changes with time. Hence, time of exposure to changing levels of tension is important in the determination of bilayer strength. Too lengthy to report here, we have recently tested the dependence of rupture tension on the time scale used to apply tension to a vesicle for most of these unsaturated PC bilayers (Evans and Ludwig, 2000). Although the results confirm the kinetic nature of the rupture process when examined over 10,000-fold change in time scale, the measurements of rupture tension varied little in the range of plus/minus an order of magnitude above/below the rate of $\sim$0.1 mN/m/s used in this study. Thus, the lysis tensions given in Table 1 and Fig. 7 represent the

levels of strength to be expected for polyunsaturated PC bilayers with 18-carbon chains in most practical situations.

APPENDIX

Analysis of vesicle area and volume

Changes in vesicle membrane area or volume were calculated from displacements in projection length inside the pipette L_p using the geometric relations for total area and volume of an aspirated vesicle. Because the pressurized shape of a fluid bilayer vesicle is a perfect sphere, the relations depend only on the diameter D_v of the vesicle-spherical segment outside the pipette, the internal diameter of the pipette D_p, and the projection length: i.e.,

(1) Hemispherical cap and cylindrical portion of the projection inside the pipette,

$$A_{cap} = \pi D_p^2/2$$

$$A_{cyl} = \pi D_p(L_p - D_p/2)$$

$$V_{cap} = \pi D_p^3/12$$

$$V_{cyl} = \pi D_p^2(L_p - D_p/2)/4$$

(2) and spherical segment of the vesicle region outside the pipette,

$$u = [1 - (D_p/D_v)^2]^{1/2}$$

$$A_{ves} = \pi D_v^2(1 + u)/2$$

$$V_{ves} = \pi D_v^3(2 + 3u - u^3)/24$$

combine to specify the total area and volume,

$$A_{tot} = A_{cap} + A_{cyl} + A_{ves}$$

$$V_{tot} = V_{cap} + V_{cyl} + V_{ves}$$

The geometric parameters (D_p, D_v, and L) were measured at the beginning of each vesicle experiment. Then, using these values, changes in either area (for the volume V_{tot} held constant) or volume (for the area A_{tot} held constant) were calculated from the measurements of displacements in projection length L_p, where the geometric constraint was used to relate the instantaneous diameter D_v of the spherical segment to projection length.

The authors thank Sid Simon and Tom McIntosh at Duke University for helpful discussions.

This work was supported by U.S. National Institutes of Health Grants GM40162 and GM08555 (to D.N.) and Canadian MRC Grant MT7477 (to E.E.).

REFERENCES

Barton, P. G., and F. D. Gunstone. 1975. Hydrocarbon chain packing and molecular motion in phospholipid bilayers formed from unsaturated lecithins. *J. Biol. Chem.* 250:4479–4476.

Davis, P. J., and K. M. W. Keough. 1983. Differential scanning calorimetric studies of aqueous dispersions of mixtures of cholesterol with some mixed-acid and single-acid phosphatidylcholines. *Biochemistry.* 22: 6334–6340.

Deryagin, B. V., and Yu. V. Gutop. 1962. Theory of the breakdown (rupture) of free films. *Kolloidn. Zh.* 24:370–374.

Evans, E., and F. Ludwig. 2000. Dynamic strengths of molecular anchoring and material cohesion in fluid biomembranes. *J. Physics: Condens. Matter.* 12:315–320.

Evans, E., and D. Needham. 1987. Physical properties of surfactant bilayer membranes: thermal transitions, elasticity, rigidity, cohesion, and colloidal interactions. *J. Phys. Chem.* 91:4219–4228.

Fettiplace, R., and D. A. Haydon. 1980. Water permeability of lipid membranes. *Physiol. Rev.* 60:510–550.

Finkelstein, A. 1987. Water Movement Through Lipid Bilayers, Pores, and Plasma Membranes: Theory and Reality. Wiley Interscience, New York.

Goldstein, B., and M. Dembo. 1995. Approximating the effects of diffusion on reversible reactions at the cell surface: ligand-receptor kinetics. *Biophys. J.* 68:1222–1230.

Hallett, F. R., J. Marsh, B. G. Nickle, and J. M. Wood. 1993. Mechanical properties of vesicles. II. A model for osmotic swelling and lysis. *Biophys. J.* 64:435–442.

Huster, D., A. J. Jin, K. Arnold, and K. Gawrisch. 1997. Water permeability of polyunsaturated lipid membranes measured by ^{17}O NMR. *Biophys. J.* 73:855–864.

Jansen, M., and A. Blume. 1995. A comparative study of diffusive and osmotic water permeation across bilayers composed of phospholipids with different headgroups and fatty acyl chains. *Biophys. J.* 68: 997–1008.

Keough, K. M. W., and N. Kariel. 1987. Differential scanning calorimetric studies of aqueous dispersions of phosphatidylcholines containing 2 polyenoic chains. *Biochim. Biophys. Acta.* 902:11–18.

Keough, K. M. W., and C. S. Parsons. 1990. Differential scanning calorimetry of dispersions of products of oxidation of 1-stearoyl-2-linoleoyl-sn-glycero-3-phosphocholine. *Biochem. Cell Biol.* 68:300–307.

Kim, R. S., and F. S. LaBella. 1987. Comparison of analytical methods for monitoring autoxidation profiles of authentic lipids. *J. Lipid Res.* 28: 1110–1117.

Koenig, B. W., H. H. Strey, and K. Gawrisch. 1997. Membrane lateral compressibility determined by NMR and x-ray diffraction: effect of acyl chain polyunsaturation. *Biophys. J.* 73:1954–1966.

Kwok, R., and E. A. Evans. 1981. Thermoelasticity of large lecithin bilayer vesicles. *Biophys. J.* 35:637–652.

Mui, B. L.-S., P. R. Cullis, E. A. Evans, and T. D. Madden. 1993. Osmotic properties of large unilamellar vesicles prepared by extrusion. *Biophys. J.* 64:443–453.

Needham, D., T. J. McIntosh, and E. A. Evans. 1988. Thermomechanical and transition properties of dimyristoylphosphatidylcholine/cholesterol bilayers. *Biochemistry.* 27:4668–4673.

New, R. R. C. 1990. Liposomes: a Practical Approach. Oxford University Press, Oxford.

Paula, S., A. G. Volkov, A. N. V. Hoek, T. H. Haines, and D. W. Deamer. 1996. Permeation of protons, potassium ions, and small polar molecules through phospholipid bilayers as a function of membrane thickness. *Biophys. J.* 70:339–348.

Rawicz, W., K. Olbrich, T. McIntosh, D. Needham, and E. Evans. 2000. Effect of chain length and unsaturation on elasticity of lipid bilayers. *Biophys. J.*

Rutkowski, C. A., L. M. Williams, T. H. Haines, and H. Z. Cummins. 1991. The elasticity of synthetic phospholipid vesicles obtained by photon correlation spectroscopy. *Biochemistry.* 30:5688–5696.

Silvius, J. R., and R. N. McElhaney. 1979. Effects of phospholipid acyl chain structure on thermotropic phase properties. 2. Phosphatidylcholines with unsaturated or cyclopropane acyl chains. *Chem. Phys. Lipids.* 25:125–134.

Xiang, T-X., and B. D. Anderson. 1997. Permeability of acetic acid across gel and liquid-crystalline lipid bilayers conforms to free-surface-area theory. *Biophys. J.* 72:223–237.

Ye, R., and A. S. Verkman. 1989. Simultaneous optical measurements of osmotic and diffusional water permeability in cells and liposomes. *Biochemistry.* 28:824–829.

Zeldovich, J. B. 1943. On the theory of new phase formation; cavitation. *Acta Physicochim. URSS.* 18:1–22.